Annexin A2 facilitates endocytic trafficking of antisense oligonucleotides

Shiyu Wang[1], Hong Sun[1], Michael Tanowitz[2], Xue-hai Liang[1,*] and Stanley T. Crooke[1]

[1]Department of Core Antisense Research, Ionis Pharmaceuticals, Inc. 2855 Gazelle Court, Carlsbad, CA 92010, USA and [2]Department of Medicinal Chemistry, Ionis Pharmaceuticals, Inc. 2855 Gazelle Court, Carlsbad, CA 92010, USA

ABSTRACT

Chemically modified antisense oligonucleotides (ASOs) designed to mediate site-specific cleavage of RNA by RNase H1 are used as research tools and as therapeutics. ASOs modified with phosphorothioate (PS) linkages enter cells via endocytotic pathways. The mechanisms by which PS-ASOs are released from membrane-enclosed endocytotic organelles to reach target RNAs remain largely unknown. We recently found that annexin A2 (ANXA2) co-localizes with PS-ASOs in late endosomes (LEs) and enhances ASO activity. Here, we show that co-localization of ANXA2 with PS-ASO is not dependent on their direct interactions or mediated by ANXA2 partner protein S100A10. Instead, ANXA2 accompanies the transport of PS-ASOs to LEs, as ANXA2/PS-ASO co-localization was observed inside LEs. Although ANXA2 appears not to affect levels of PS-ASO internalization, ANXA2 reduction caused significant accumulation of ASOs in early endosomes (EEs) and reduced localization in LEs and decreased PS-ASO activity. Importantly, the kinetics of PS-ASO activity upon free uptake show that target mRNA reduction occurs at least 4 hrs after PS-ASOs exit from EEs and is coincident with release from LEs. Taken together, our results indicate that ANXA2 facilitates PS-ASO trafficking from early to late endosomes where it may also contribute to PS-ASO release.

INTRODUCTION

Antisense oligonucleotides (ASOs) that mediate RNA cleavage by RNase H1 are broadly used as biological tools and therapeutic agents. To confer resistance to degradation by nucleases and enhance pharmacological properties, ASOs generally have phosphorothioate (PS) backbones and terminal residues are modified at the 2′-position of the ribose (1). PS-ASOs enter cells mainly via endocytotic pathways in the absence of transfection reagents (2,3). PS-ASOs that enter cells through this so-called free uptake route can lead to sequence-specific cleavage of target RNAs in both cytoplasm and nucleus (4). Internalization of PS-ASOs is a complex process that is not fully understood. There is evidence that uptake occurs by receptor-mediated endocytosis at low PS-ASO concentrations (<1 μM) and by fluid phase endocytosis at high PS-ASO concentrations (>4 μM) (5). In primary hepatocytes, PS-ASOs are endocytosed through a clathrin- and caveolin-independent, but AP2M-dependent endocytic process (3). The route of internalization appears to affect the ultimate activity of ASOs. For example, PS-ASOs conjugated with triantennary N-acetyl galactosamine enter cells through a process mediated by the asialoglycoprotein receptor (ASGPR) and exhibit higher activity than do unconjugated PS-ASOs (6).

PS-ASOs are trafficked through early endosomes (EEs), late endosomes (LEs), and lysosomes (7). Although the effect of intracellular trafficking of PS-ASOs on their activity is not fully understood (3,8,9), it has been proposed to occur via both productive and non-productive pathways (3,9). A large portion of internalized PS-ASOs accumulate in LEs and lysosomes and remain inactive (non-productive); a fraction is released to the cytosol and nucleus and act on target RNAs (productive). Different models have been proposed to explain PS-ASO escape from endosomes and lysosomes (10). For example, membrane fusion that occurs constantly during the trafficking process could create local stress, resulting in formation of non-bilayer lipid domains with increased permeability allowing PS-ASO release (2,11,12). Protein binding to the membrane may change its conformation, also leading to PS-ASO release (2,13,14). Since the pharmacological effects of PS-ASOs gradually increase over several hours in cell-based assays, it is likely that at least some productive PS-ASO release stems from low levels of continuous leakage from membrane-enclosed vesicles.

In our previous studies of PS-ASO-binding proteins, we identified annexin A2 (ANXA2) as one of the dozens of intracellular proteins that interact with PS-ASOs and affect PS-ASO activity (15). The binding of PS-ASOs to most

*To whom correspondence should be addressed. Tel: +1 760 603 3816; Fax: +1 760 603 4561; Email: Lliang@ionisph.com

proteins is mediated in part by the PS backbone because ASOs with a phosphodiester (PO) backbone have a much weaker binding than PS backbone to cellular proteins. In addition, 2′-modification as well as sequence of PS-ASOs can be important for binding to some proteins (15–17). ANXA2 is a member of the annexin family, which contains 14 proteins in humans. Annexin proteins are involved in endocytosis, exocytosis, membrane trafficking and remodeling, and cytoskeleton interactions (18,19). Annexins interact with anionic phospholipids in a Ca^{2+}-dependent manner (20), and different annexin proteins bind to distinct phospholipids in different intracellular environments (21–23). ANXA2 mainly binds phosphatidylethanolamine (PE), phosphatidylinositol bisphosphate PI (4,5) P2, and cholesterol (19). ANXA2 is both membrane-associated and cytosolic (24). Membrane-associated ANXA2 is predominantly present in EEs, although some ANXA2 also localizes to the plasma membrane, as well as being found extracellularly (25,26). ANXA2 exists either as a monomer or as a heterotetrameric complex partnered with S100 calcium-binding protein A10 (S100A10) (27). ANXA2 also plays an important role in the biogenesis of multivesicular bodies, which bud from EEs and are able to mature to the LEs (28). ANXA2 mediates EGFR trafficking from early to late endosomes (29).

We previously showed that ANXA2 interacts with PS-ASOs, is important for PS-ASO antisense activity, and co-localizes with PS-ASOs in LEs (15). Here we describe a further analysis of the roles of ANXA2 in PS-ASO intracellular trafficking. We found that reduction of ANXA2 levels delayed PS-ASO trafficking from early to late endosomes and resulted in accumulation of PS-ASOs in EEs. Interestingly, ANXA2 co-localized with ASOs inside LEs, suggesting that ANXA2 accompanies ASOs as it moves from early to late endosomes. This raises the possibility that ANXA2 is directly involved in PS-ASO release from LEs.

MATERIALS AND METHODS

Antibodies, siRNAs, ASOs and quantitative real-time PCR (qRT-PCR) primer probe sets are listed in Supplementary Data.

Cell culture, transfection, PS-ASO free uptake and activity

HeLa, Hek293, HepG2 and A431 cells were grown according to the protocols provided by the American Type Culture Collection (ATCC, Manassas, VA, USA). MHT cells were grown as described previously (3). Cells were seeded at 70% confluency one day before transfection or drug treatment. siRNAs were transfected at 3 nM final concentration using RNAiMAX (Life Technologies, Carlsbad, CA, USA), according to the manufacturer's protocol. At 48 h after siRNA transfection, cells were re-seeded in either 96-well plates or collagen-coated dishes (MatTek, Ashland, MA, USA) at 50% confluency. Cells were incubated for 16 hrs, and then the PS-ASO activity assay or immunofluorescence analysis was performed.

RNA preparation and qRT-PCR

Total RNA was prepared using an RNeasy mini kit (Qiagen, Valencia, CA, USA) from cells grown in 96-well plates (∼10 000 cells per well). qRT-PCR using TaqMan primer probe sets were performed essentially as described previously (15). Briefly, ∼50 ng total RNA in 5 μl water was mixed with 0.3 μl primer probe sets containing forward and reverse primers (10 μM of each) and fluorescently labeled probe (3 μM), 0.3 μl RT enzyme mix (Qiagen), 4.4 μl RNase-free water, and 10 μl of 2× PCR reaction buffer in a 20 μl reaction. Reverse transcription was performed at 48°C for 10 min, 40 cycles of PCR were conducted at 94°C for 20 s, and 60°C for 20 s within each cycle, using StepOne Plus RT-PCR system (Applied Biosystems, Phoenix, AZ, USA). The mRNA levels were normalized to the amount of total RNA present in each reaction as determined for duplicate RNA samples by Ribogreen assay (Life Technologies).

Subcellular fractionation

A431 cells, either untreated or treated with 2 μM indicated PS-ASOs for 16 hrs, were collected in hypotonic homogenization buffer (3 mM imidazole, 0.25 M sucrose and protease inhibitor cocktail). Approximately 1×10^8 cells were homogenized using Balch homogenizer (Heidelberg, Germany) in 1 ml hypotonic homogenization buffer at 4°C, and a post-nuclear supernatant was prepared using centrifugation at 4500g. The supernatant was then adjusted to 40.6% sucrose using 62% sucrose at the bottom of an SW41 ultra-centrifugation tube (Beckman, Brea, CA, USA) in no >2 ml. We then sequentially overlaid the sample with 3.5 ml of 35% and 25% sucrose solutions and then filled the tube with homogenization buffer. The gradient was centrifuged for 3 hrs at 45 000g. The early endosomal fraction was collected from the interface of the 35% and the 25% sucrose layers, and the late endosomal fraction was collected from the interface of the 25% sucrose gradient and homogenization buffer. Each fraction was diluted with homogenization buffer and pelleted by centrifugation for 1 hr at 4°C, 100 000g, using a SW55 rotor. The pellet was either used directly in a western blot analysis, or was incubated in 2 M NaCl in PBS for 30 min. Proteins that were released or associated with membrane after incubation in 2 M NaCl in PBS were precipitated by centrifugation prior to western blot analysis.

Immunoprecipitation

A431 cells either untreated or treated with 2 μM indicated PS-ASO for 16 hrs were lysed in IP buffer (Life Technologies). Total proteins were collected by centrifugation followed by incubation with S100A10 antibody or ANXA2 antibody and Protein G agarose beads (Life Technologies). Beads were washed three times with IP buffer then eluted using SDS sample buffer (Life Technologies) for western blotting analysis and silver staining (Sigma).

Immunofluorescence staining

Cells were fixed with 4% paraformaldehyde for 30 min at room temperature and were permeabilized with 0.05% saponin (Sigma) in PBS for 5 min. Cells were treated with

blocking buffer (1 mg/ml BSA in PBS) for 30 min and then incubated with primary antibodies (1:100–1:200 in blocking buffer) at room temperature for 2–4 hrs, or at 4°C overnight. After three washes using 0.1% Triton in PBS, cells were incubated with fluorescently labeled secondary antibodies (1:200 in blocking buffer) at room temperature for 1–2 hrs. After washing, slides were mounted with Prolong Gold anti-fade reagent with DAPI (Life Technologies) and imaged using a confocal microscope (Olympus FV-1000). Images were quantified using software of FV10-ASW 3.0 viewer.

Protein isolation and western blotting

Cells were lysed, and samples were incubated at 4°C for 30 min in RIPA buffer (50 mM Tris–HCl, pH 7.4, 1% Triton X-100, 150 mM NaCl, 0.5% sodium deoxycholate, and 0.5 mM EDTA). Proteins were separated by PAGE using 6–12% NuPAGE Bis-Tris gradient Gels (Life Technologies) and electroblotted onto PVDF membranes using the iBLOT transfer system (Life Technologies). The membranes were blocked with 5% non-fat dry milk in PBS at 4°C for 30 min. Membranes were then incubated with primary antibodies (Supplemental Data) at room temperature for 1 hr. After three washes with PBS, the membranes were incubated with appropriate HRP-conjugated secondary antibodies (1:2000) at room temperature for 1 hr to develop the image using ECL reagents (Abcam, Cambridge, MA, USA).

Affinity selection of PS-ASO-binding proteins

Proteins associated with a biotinylated PS-ASO (IONIS ID 386652) were isolated using neutravidin beads from HeLa cell lysate. Co-isolated proteins were eluted by competition using either a PS-ASO (IONIS ID: 116847) or a PO-ASO (IONIS ID 364617) as described previously (16). The eluted proteins were analyzed by SDS-PAGE and ANXA2 protein was detected by western blotting analysis.

Flow cytometry

Indicated Cy3-labeled PS-ASOs were added to A431 cell culture. After 3 hrs, cells were washed with PBS, trypsinized, and resuspended in PBS supplemented with 3% fetal bovine serum for analysis by flow cytometry using a BD CellQuest Pro system (BD Biosciences, San Jose, CA, USA).

RESULTS

ANXA2 co-localizes with PS-ASO in different cell types

We previously found that ANXA2 co-localized with PS-ASOs in LEs and reduction of ANXA2 decreased PS-ASO activity in HeLa cells (15). To determine the generality of this observation, we examined co-localization of PS-ASOs with ANXA2 in different cells of different types and from different species. The same Cy3-labeled PS-ASO used in the previous study (IONIS ID 446654) was incubated for 15 hrs with human Hek293, HepG2 and A431 cells, and with mouse MHT cells. Immunofluorescence staining showed that in the presence of PS-ASOs, ANXA2 was observed in dot-like structures in the cytoplasm that co-localized with ASOs in LEs in all tested cell types (Figure 1A). This pattern was similar to what was observed in HeLa cells (15). The number of co-stained loci was also quantified and ANXA2 was present in more than 40% LEs in all cell lines studied (data not shown). In the absence of ASO treatment, ANXA2 was evenly distributed in the cytoplasm as described previously (Figure 1A, lower panel). Thus, ANXA2 co-localizes with PS-ASOs in a variety of cell types.

ANXA2 is important for ASO activity in different cell types

To determine whether ANXA2 is also important for PS-ASO activity in different cell types, ANXA2 protein levels were reduced transiently by treating human A431 cells with an siRNA designed to target *ANXA2* mRNA (Figure 1B). Cells treated with a control siRNA (targeting *luciferase* mRNA) or *ANXA2* siRNA were incubated with PS-ASOs targeting *Drosha* mRNA or *Malat1* long noncoding RNA. After 15 hrs, the levels of the targeted RNAs were quantified by qRT-PCR (Figure 1C and D). Reduction of ANXA2 significantly reduced the activity of PS-ASOs in A431 cells, consistent with our previous results that the presence of ANXA2 is important for PS-ASO activity in HeLa cells (15). Similar reduction in PS-ASO activity was observed when ANXA2 levels were reduced using two different siRNAs in mouse MHT cells (Figure 1E–G). We have also generated a stable HeLa cell line that overexpresses DKK-tagged ANXA2 and examined how overexpression of ANXA2 altered PS-ASO activity. In these cells, the levels of overexpressed ANXA2 were almost 3-fold more than endogenous ANXA2; however, that did not increase PS-ASO activity (Supplementary Figure S1), suggesting that ANXA2 overexpression itself is not sufficient to enhance PS-ASO activity. Nonetheless, these results further demonstrate that ANXA2 co-localizes with PS-ASOs and reduction of ANXA2 decreases PS-ASO activity in different human and mouse cell types.

ANXA2 is not required for PS-ASO internalization

Since ANXA2 can be localized at the cytoplasmic face of the plasma membrane (24), we reasoned that ANXA2 could directly contribute to PS-ASO internalization, and therefore we analyzed the effect of ANXA2 reduction on levels of PS-ASO internalization. Treatment of HeLa cells with *ANXA2* siRNA significantly reduced ANXA2 protein levels and decreased PS-ASO activity (Figure 2A–C), as previously demonstrated (15). HeLa cells treated with control or *ANXA2* siRNA were incubated with Cy3-labeled PS-ASOs (IONIS ID 446654) for 3 hrs, and the cellular levels of PS-ASOs were determined by FACS analyses (Figure 2D). The levels of internalized PS-ASOs were comparable in control and ANXA2-deficient cells. This indicates that ANXA2 does not affect PS-ASO uptake. This conclusion was supported by our observation that incubation of HeLa cells with three different ANXA2 antibodies did not affect PS-ASO uptake (data not shown). Thus, ANXA2 appears to influence PS-ASO activity through effects on intracellular events.
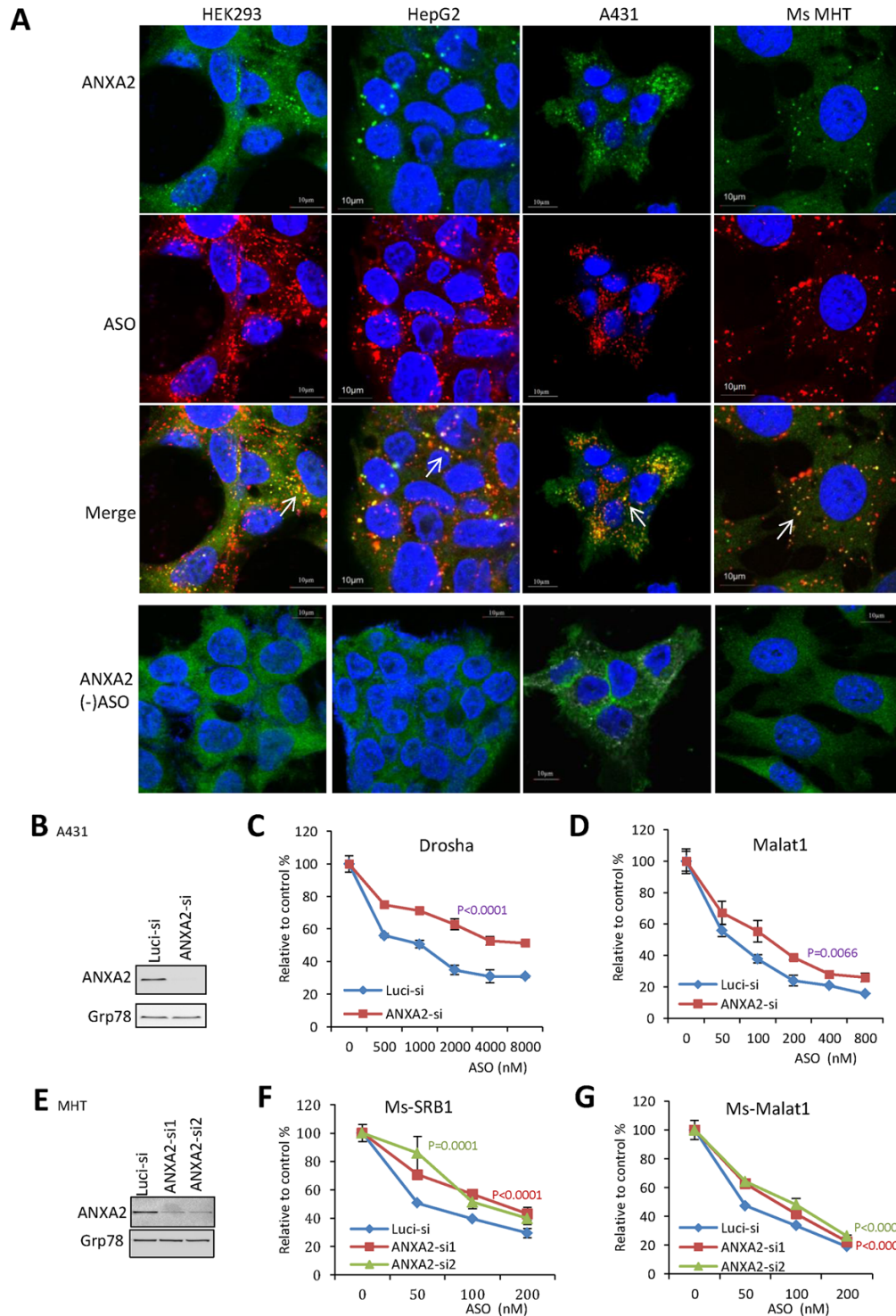
Figure 1. ANXA2 localizes to LEs in different cell types treated with PS-ASOs. (**A**) Representative immunofluorescence images of indicated cells stained for ANXA2 (green) and PS-ASO (red). Cells were incubated with 2 μM PS-ASO (IONIS ID 446654) for 8 hrs prior to staining. The lower panels are images of cells not treated with PS-ASO stained for ANXA2. Nuclei were stained with DAPI (blue). Scale bars, 10 μm. Arrows indicate the co-localization of ANXA2 and PS-ASO. (**B**) Western analyses for ANXA2 protein in A431 cells treated with control luciferase siRNA (Luci-si) or *ANXA2*-specific siRNA (ANXA2-si). Grp78 served as a control for loading. (**C** and **D**) Cells treated with control luciferase siRNA (blue) or *ANXA2*-specific siRNA (red) were incubated with PS-ASOs targeting either *Drosha* or *Malat1* RNAs for 16 hrs, and levels of (**C**) Drosha and (**D**) Malat1 RNA were analyzed by qRT-PCR. Results were presented relative to no PS-ASO control. (**E**) ANXA2 protein levels in MHT cells treated with control siRNA (Luci-si) or with siRNAs specific for mouse *ANXA2* mRNA (ANXA2-si1 and ANXA2-si2). Grp78 served as a loading control. (**F** and **G**) MHT cells treated with control siRNA (Luci-si, blue) or ANXA2 siRNAs (ANXA2-si, red; or ANXA2-si2, green) were incubated with PS-ASOs targeting SRB1 mRNA (F) or Malat1 RNA (G), and the RNA levels were analyzed by qRT-PCR. Results were presented relative to no PS-ASO control. The error bars for qRT-PCR assay represent standard deviations from three independent experiments. *P*-values were calculated based on two-tailed, paired *t*-test.
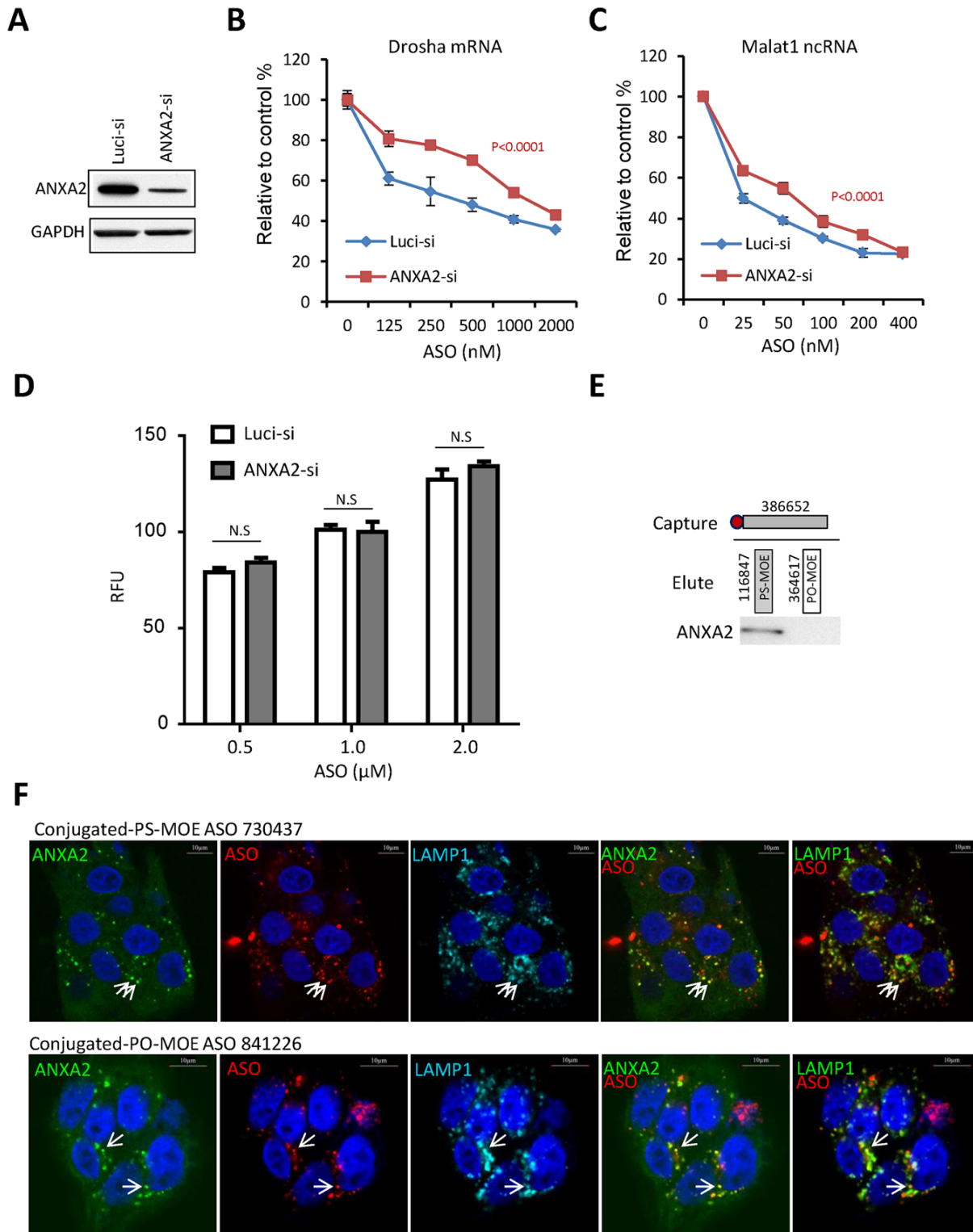
Figure 2. Reduction of ANXA2 does not affect PS-ASO uptake. (**A**) Western analysis for ANXA2 protein levels in control HeLa cells or cells treated with an *ANXA2*-specific siRNA. GAPDH served as a loading control. (**B** and **C**) Control (Luci-si) or *ANXA2* siRNA (ANXA2-si)-treated HeLa cells were incubated with PS-ASOs targeting either *Drosha* or *Malat1* RNA for 16 hrs, and RNA levels were determined using qRT-PCR. Results were presented relative to no PS-ASO control. (**D**) HeLa cells treated with control (Luci-si, white bars) or *ANXA2* siRNA (ANXA2-si, gray bars) were incubated with Cy3-labeled PS-ASO (IONIS ID 446654) for 3 hrs. PS-ASO uptake was analyzed by flow cytometry; results were presented as relative fluorescence units (RFU). The error bars represent standard deviations from three independent experiments. (**E**) Western analysis for ANXA2 protein co-isolated with PS-ASO (IONIS ID 116847) and PO-ASO (IONIS ID 364617). (**F**) Representative images of immunofluorescence staining of ANXA2 and LAMP1 in HepG2 cells incubated with 2 μM GalNAc-PS-ASO (upper panel) or GalNAc-PO-ASO (lower panel) for 8 hrs. Arrows indicate the co-localization of ANXA2, PS-ASO, and LAMP1. Scale bars, 10 μm.

Co-localization of ANXA2 and PS-ASO is not driven by a direct interaction

Previously we demonstrated that certain PS-ASO-binding proteins, such as TCP1β, impact PS-ASO activity through a direct interaction with the PS-ASOs (16). Affinity selection analyses showed that ANXA2 bound to biotinylated PS-ASOs in cell lysates (15). Therefore, it is possible that co-localization of ANXA2 with PS-ASOs is mediated by a direct interaction with ANXA2. To test this possibility, cells were treated with Cy3-labeled PS-ASOs containing different 2′-modifications such as locked-nucleic-acid (LNA), constrained-ethyl-bicyclic-nucleic-acid (cEt), 2′-fluoro (F), or deoxynucleotides (DNA) that are known to bind proteins to different extents (15). ANXA2 was localized to LEs in cells treated with all PS-ASOs irrespective of 2′ modification (Supplementary Figure S2A). PS/MOE ASOs with different sequences detected using PS-ASO specific antibody were also found to co-localize with ANXA2 (Supplementary Figure S2B). Quantification of co-stained loci between ANXA2 and these PS-ASOs further confirmed that 2′-modifications or sequences have no significant effect on their co-localization (data not shown).

We have shown previously that PS-ASOs bind with much higher affinity to intracellular proteins than PO-ASOs (15). When cellular proteins bound with a biotinylated PS-MOE ASO were eluted by competition using PS- or PO-ASOs of otherwise the same sequence and chemistry, ANXA2 was only eluted with PS-ASOs, but not with PO-ASOs, as detected by western analyses (Figure 2E). This suggests that ANXA2 does not significantly interact with PO-ASOs. PO-ASOs are not efficiently taken up by cells in the absence of transfection reagent (30). However, PO-ASOs conjugated with triantennary N-acetyl galactosamine (GalNAc) can enter cells via ASGPR-mediated endocytosis pathway (6). We thus incubated GalNAc-conjugated PO-ASO and PS-ASO with HepG2 cells, which express ASGPR (6), and the localization of ANXA2 was determined by immunofluorescence staining. Interestingly, ANXA2 co-localized with both the GalNAc-PS-ASO and the GalNAc-PO-ASO in LEs (Figure 2F). Quantification of co-stained loci between ANXA2 and PS-ASOs or PO-ASOs did not show any significant difference (∼ 7 loci per cell, data not shown). As PO-ASOs do not interact with ANXA2 but still recruit ANXA2 to LEs and the structure activity relationship of binding to ANXA2 by PS-ASOs do not correlate with co-localization, a direct interaction between ANXA2 and the ASOs is probably not required for the co-localization of ANXA2 with ASO in LEs.

Localization of ANXA2 to LEs in cells treated with PS-ASO is associated with intracellular trafficking of PS-ASO

Upon treatment of cells with PS-ASOs, ANXA2 relocates from the cytoplasm to LEs, and co-localization of PS-ASOs and ANXA2 was observed in LEs but not in EEs (15). If the ANXA2 localization to LEs is correlated with ASO intracellular trafficking, amount of ANXA2 in LEs should correlate with the amount of PS-ASO transported to LEs. To test this possibility, ANXA2 localization was monitored by immunofluorescence staining in HeLa cells incubated for 8 hrs with different concentrations of Cy3-labeled PS-ASOs

(IONIS ID 446654). ANXA2 staining of LEs, indicated by staining with Rab7, was increased as the dose of PS-ASO increased (Figure 3A).The number of co-stained loci quantitatively increased from ∼2 to at least ∼40 per cell when the PS-ASO concentration was increased from 0.25 to 2 μM (Figure 3B).

The localization of ANXA2 to LEs was not due to the fluorescent label used in these experiments, as increased co-localization was observed in cells pre-treated with 2 μM unlabeled PS-ASO (IONIS ID 116847, the same chemistry and sequence as IONIS ID 446654 without Cy3 dye) for 4 hrs, followed by addition of 2 μM Cy3-labeled PS-ASO for an additional 4 hrs (Supplementary Figure S3). The Cy3-independence of ANXA2 and PS-ASO co-localization was also confirmed using a PS-ASO antibody (Supplementary Figure S2B). Together, these results suggest that ANXA2 is recruited to LEs in the presence of PS-ASO, suggesting that it is involved in intracellular trafficking of PS-ASOs.

We previously found that co-localization of ANXA2 and PS-ASO was not obvious at 2 hrs after treatment of cells with PS-ASOs was initiated; co-localization was apparent at 4 hrs (15). Here we analyzed immunofluorescence staining of ANXA2 in HeLa cells over a more detailed time course from 1 to 4 hrs after PS-ASO incubation (Figure 3C). We observed small loci that co-stained for ANXA2 and PS-ASOs after 1 hr, and the numbers and sizes of the co-stained loci increased over time. The co-stained loci were quantified and ∼4, ∼21 and ∼32 loci per cell were observed after incubation with PS-ASOs for 1, 2 and 3 hrs, respectively. Thus, these results suggest that ANXA2 is recruited to LEs during PS-ASO intracellular trafficking and that accumulation in LEs correlates with levels of PS-ASOs in the organelle.

The effect of ANXA2 on PS-ASO activity is independent of its partner protein S100A10

ANXA2 is known to function either as a monomer or a heterotetramer complexed with S100A10. Monomeric ANXA2 and heterotetrameric ANXA2 with S100A10 are preferentially localized to EEs and to the subplasmalemmal region, respectively (31). To ascertain whether the effects of ANXA2 on PS-ASO activity are mediated by S100A10, we first determined whether S100A10 is recruited to LEs by PS-ASOs. Immunofluorescence staining was performed in HeLa cells treated with PS-ASOs. In the absence of PS-ASO treatment, S100A10 was uniformly distributed throughout the cytoplasm (Figure 4A, upper panel). Upon treatment of cells with PS-ASOs, S100A10 was enriched in LEs containing ANXA2 and PS-ASOs (Figure 4A, lower panels). Further, the interactions between ANXA2 and S100A10 were not affected by the presence of PS-ASOs, as an ANXA2 antibody precipitated S100A10 similarly from cell lysates of untreated and PS-ASO-treated cells (Figure 4B, panel a). In addition, other ANXA2-associated proteins immunoprecipitated by ANXA2 antibody were also comparable in silver stain gel from cell lysates of untreated and PS-ASO-treated cells (Figure 4B, panel b). Therefore, PS-ASOs do not affect ANXA2 interaction with other proteins.

To determine if the effects of ANXA2 on PS-ASO activity are mediated by S100A10, A431 cells were treated with two different siRNAs targeting *S100A10*; both de-
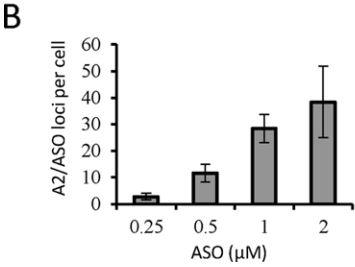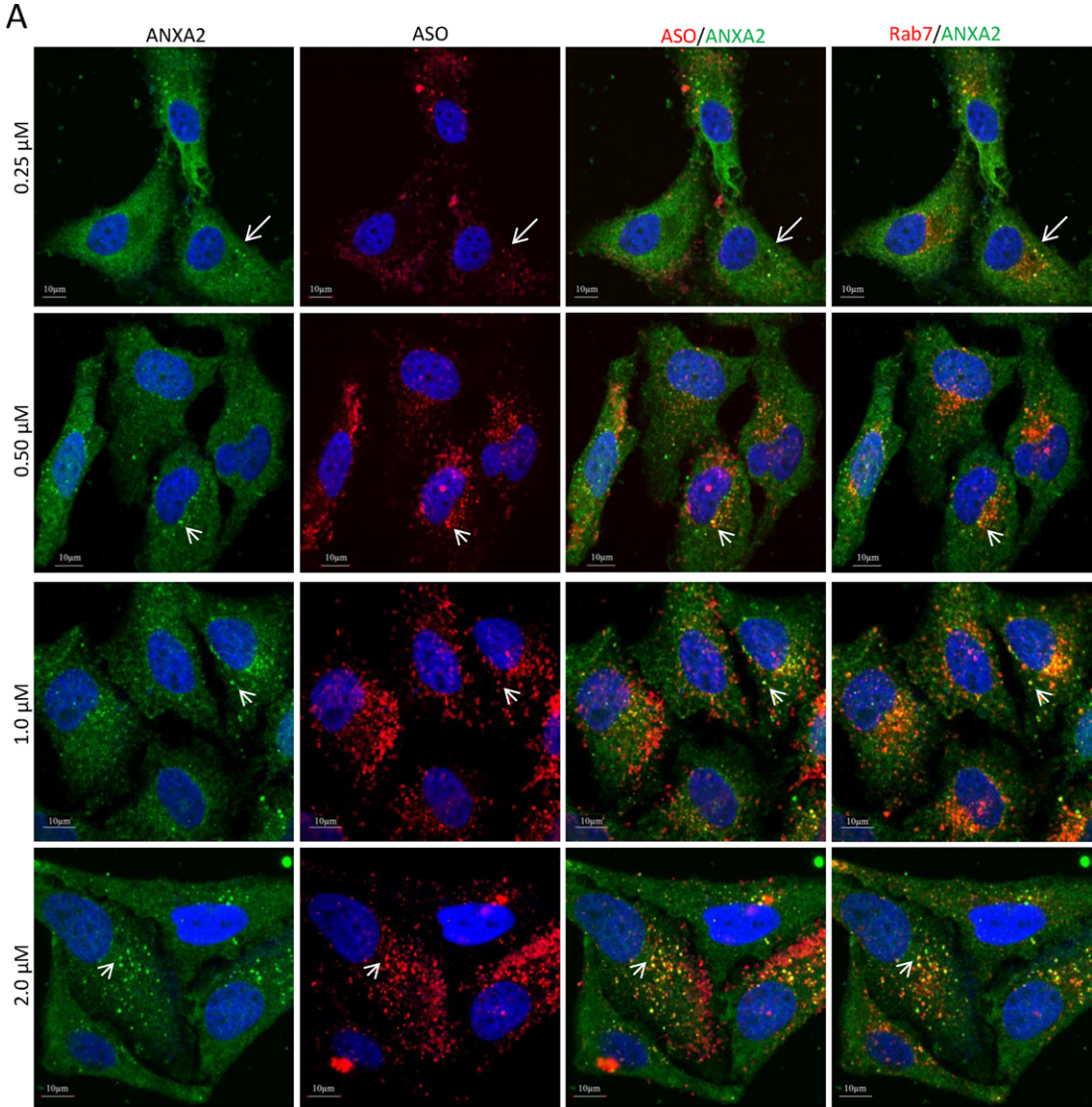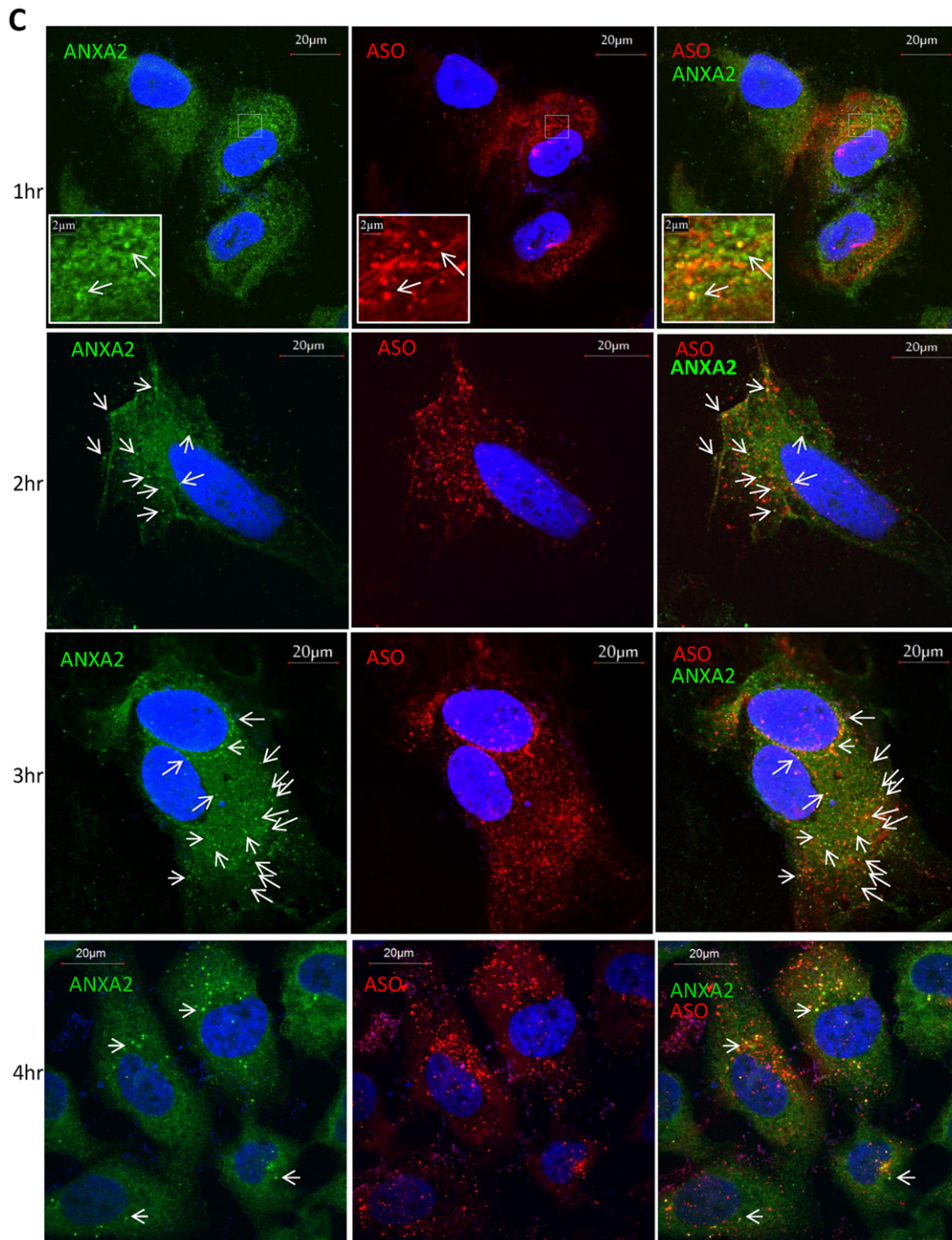
Figure 3. ANXA2 localization to LEs is PS-ASO dose-dependent and occurs shortly after PS-ASO treatment begins. (**A**) Representative images of immunofluorescent staining for ANXA2 and Rab7 in HeLa cells incubated with different concentrations of Cy3-labeled PS-ASO (IONIS ID 446654) for 8 hrs. Images for PS-ASO (red) and ANXA2 (green) were merged to show the co-localization. Merged images for Rab7 (red) and ANXA2 (green) were shown in right panels. The arrow indicates co-localization of PS-ASO, ANXA2, and Rab7 in LEs. The nuclei were stained with DAPI (blue). Scale bars, 10 μm. (**B**) Quantification of ANXA2-enriched loci per cell. The average number of loci in 20 cells is plotted as a function of PS-ASO concentration. The error bars represent standard deviations. (**C**) ANXA2 co-localization with PS-ASOs in HeLa cells incubated with 2 μM Cy3-labeled PS-ASO for different times. The co-localization of ANXA2 with PS-ASOs is exemplified with arrows. Scale bars, 20 μm. In magnified images, scale bars are 2 μm.
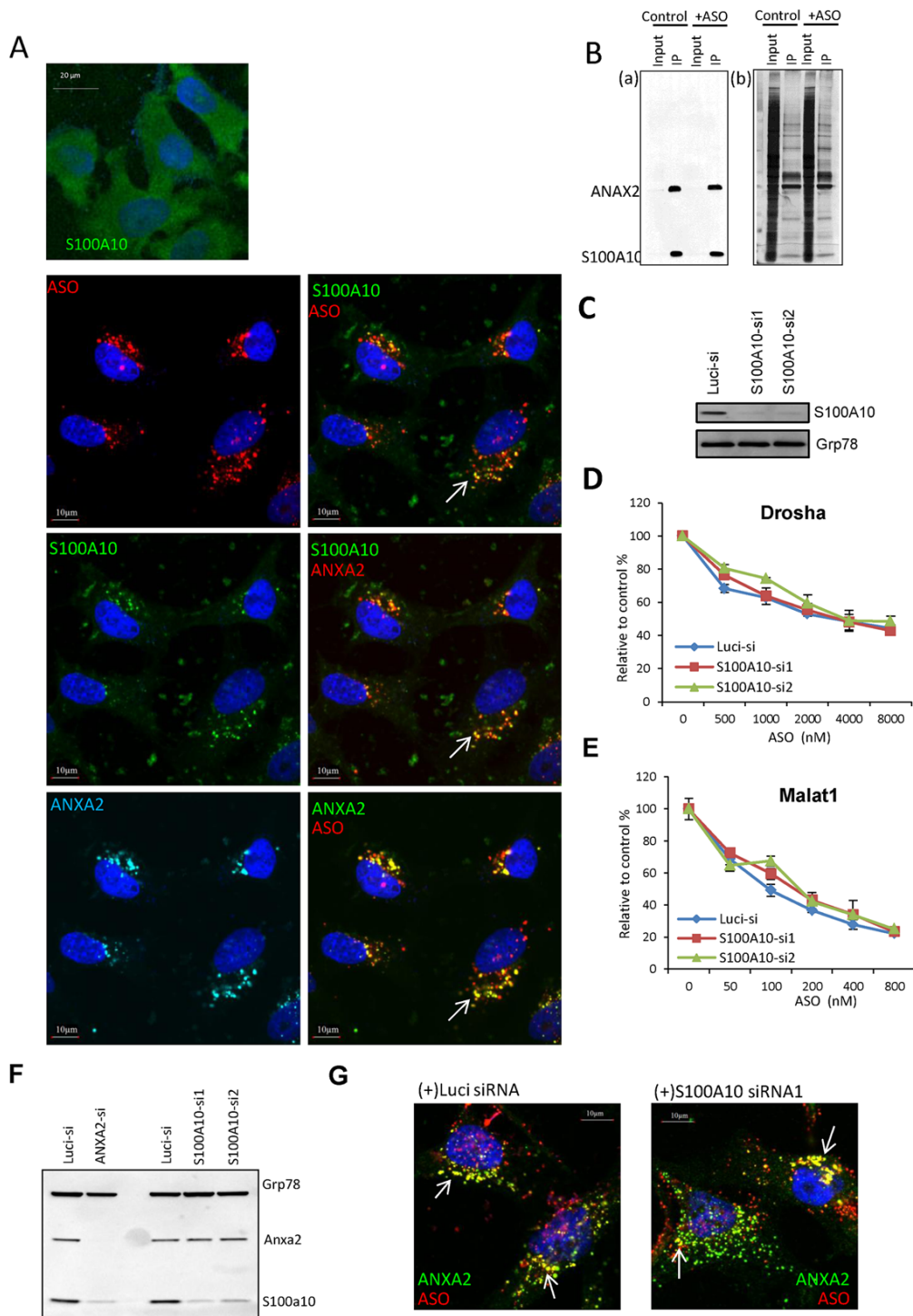
Figure 4. ANXA2 and PS-ASO co-localization is independent of S100A10. (**A**) S100A10 was stained in control HeLa cells (upper panel) or cells incubated with 2 μM Cy3-labeled PS-ASO for 8 hrs (lower panels: scale bar, 10 μm). S100A10 co-localization with PS-ASO and ANXA2 is exemplified using an arrow. (**B**) Western blot for ANXA2 and S100A10 recovered from lysates of either control or PS-ASO-treated cells by immunoprecipitation with an ANXA2 antibody (a). Silver stained SDS-PAGE gel for ANXA2-associated proteins immunoprecipitated with an ANXA2 antibody (b). Cells were treated with 2 μM PS-ASO (IONIS ID 116847) for 16 hrs; co-immunoprecipitated (IP) proteins and 10% of input lysate (input) were analyzed. (**C**) Western analysis for S100A10 protein levels in HeLa cells treated with either a *luciferase* siRNA (Luci-si) or two different siRNAs specific for *S100A10* mRNA (S100A10-si). Grp78 served as a loading control. (**D** and **E**) Cells treated with control (blue) or siRNAs for *S100A10* (S100A10-si1, red; S100A10-si2, green) were incubated with PS-ASOs targeting either *Drosha* (D) or *Malat1* (E) for 16 hrs, and the RNA levels were quantified using qRT-PCR. The error bars represent standard deviations from three independent experiments. (**F**) Western analysis for ANXA2 and S100A10 proteins in cells treated with indicated siRNAs. Grp78 served as a loading control. **G**) Immunofluorescence staining of ANXA2 protein in cells treated with control siRNA (left panel) or S100A10 siRNA (right panel) then with Cy3-PS-ASO for 8 hrs. The arrows indicate co-localization of ANXA2 (green) and PS-ASO (red). Nuclei were stained with DAPI (blue). Scale bars, 10 μm.

creased S100A10 protein levels by more than 90% (Figure 4C). Reduction of *S100A10* had no significant effect on PS-ASO activity, as demonstrated by qRT-PCR analyses for *Drosha* mRNA or *Malat1* RNAs in control or *S100A10*-deficient cells incubated with the *Drosha*- or *Malat1*-specific ASOs (Figure 4D and E). We note that ANXA2 reduction decreased S100A10 protein levels, whereas reduction of S100A10 did not affect the levels of ANXA2 protein (Figure 4F), consistent with previous observations (32,33). These results indicate that ANXA2, but not S100A10, impacts PS-ASO activity. Importantly, reduction of S100A10 did not block the localization of ANXA2 to LEs in cells treated with PS-ASOs (Figure 4G). These results indicate that ANXA2 monomer, but not ANXA2 heterotetramer, is important for PS-ASO activity.

LE-associated ANXA2 is resistant to high salt wash

ANXA2 associated with the EE membrane mediates the interaction between the membrane and actin that is critical for LE biogenesis (28). Given the membrane binding property of ANXA2 (20), it is likely that ANXA2 binds to the LE membrane after PS-ASOs are loaded to it. The PS-ASOs may alter lipid composition of the late endosomal membrane, revealing a species preferentially bound by ANXA2. We reasoned that if lipid signature is altered, other annexin proteins might also be recruited to endosomes that have entrapped PS-ASOs, because each annexin preferentially binds a certain negatively charged lipid species. We evaluated localization of the annexins ANXA1, ANXA3, ANXA4, ANXA5, ANXA6, ANXA7, ANXA8 and ANXA10 in untreated cells and in cells that had been treated with PS-ASOs. No differences in localization were observed for most of these proteins in the presence and absence of PS-ASOs (data not shown). The exceptions were ANXA3 and ANXA4, two proteins with unknown functions in endosomal biogenesis. These two annexins were detected in LEs in cells treated with PS-ASOs but diffusely stained the cytoplasm in untreated cells (Supplementary Figure S4). The loci co-stained with PS-ASOs and ANXA3 or ANXA4 were less intense and in fewer LEs than those co-stained with PS-ASOs and ANXA2. Further, reduction of ANXA3 and ANXA4 levels by siRNA treatment did not affect ASO activity (Supplementary Figure S5). This implies that LE re-localization of ANXA3 and ANXA4 did not significantly affect PS-ASO release, likely due to their weak interaction with LE membrane or marginal recruitment to LEs as compared with ANXA2 (see below). Nonetheless, these results raise the possibility that PS-ASOs alter the lipid signature of the late endosomal membrane, and that ANXA2 could be recruited to the surface of LE membrane due to altered lipid signature.

To determine whether ANXA2 is present on the surface of endosomes or internalized, we used ultracentrifugation in step sucrose gradients to isolate early and late endosomes from cells treated or not treated with PS-ASOs. The isolated fractions were first subjected to western analyses to determine their purity. Rab5 (a marker of EEs) and Alix (a marker of LEs) were only enriched in early and late endosomal fractions, respectively, and about 75% and 25% of ANXA2 was localized in the early endosomal fraction and

late endosomal fraction in control cells (Figure 5A), consistent with previous reports (34). As expected, PS-ASO treatment indeed increased the abundance of ANXA2 in the LEs: In the presence of PS-ASOs, >35% of ANXA2 was found in LEs. As most ANXA2 still remained in EEs even in the presence of PS-ASO treatment, this suggests an unambiguous role of ANXA2 in EEs for intracellular trafficking. Compared with ANXA2, ANXA3 and ANXA4 were not significantly enriched in EEs and redistribution of them to LEs is also marginal. This suggests that the interactions of these two proteins with LEs are relatively weak, consistent with their dispensable role in PS-ASO activity.

Next, the isolated late endosomal fractions were washed with a high concentration of salt (2 M NaCl) to break electrostatic interaction between proteins and membranes, with the rational that this treatment would release membrane-associated ANXA2. The proteins in membrane pellets and wash were analyzed by western blotting (Figure 5B). About 20% of ANXA2 dissociated from the LE membranes of control cells and ~30% was released from PS-ASO-treated cells. This result implies that at least a certain portion of ANXA2 protein is recruited to the LE membrane surface when PS-ASOs are present. No significant release of LAMP1 was detected from either sample. In contrast, ~50% of Alix, which is known to be associated with the membranes of LEs, was released from the late endosomal membrane by the high salt wash.

ANXA2 can be co-localized with PS-ASOs inside LEs

As a lipid binding protein, ANXA2 has been detected in the inner surface of artificial intraluminal vesicles (24). Since we were not able to completely wash ANXA2 off LE membranes, it is possible that ANXA2 is also inside of LEs where it co-localizes with PS-ASOs. To test the possibility, HeLa cells were incubated with Cy3-labeled PS-ASOs for 8 hrs and then stained for ANXA2 and LAMP1. Some cells contained enlarged LEs with open interior spaces enclosed by LAMP1 (Figure 6A). PS-ASOs were observed inside these LEs in a scattered, dot-like pattern. ANXA2 was also detected, though with a relatively weak signal, co-localized with PS-ASOs inside these LAMP1-enclosed structures. This observation suggests that PS-ASOs and ANXA2 exist in sub-structures within the LEs, likely intraluminal vesicles (ILVs).

To confirm that ANXA2 and PS-ASOs are inside limiting membrane structures of LEs, we enlarged the LEs using pharmacological tools. Cells were first treated with PS-ASOs for 8 hrs and were next treated with U18666A, which inhibits cholesterol transport out of endosomes and leads to enlarged LEs (35). As expected, U18666A treatment increased the sizes of LEs, resulting in a distinguishable inner space surrounded by LAMP1-stained membranes. ANXA2 co-localized with PS-ASOs were observed inside these enlarged endosomes (Figure 6B), suggesting that ANXA2 can traffic together with PS-ASOs to LEs. Together, our results indicate that in addition to LE membrane surface localization, at least part of ANXA2 is co-localized with PS-ASOs inside LEs, which may traffic together with PS-ASOs from EEs. Therefore, late endosomal ANXA2 could change its
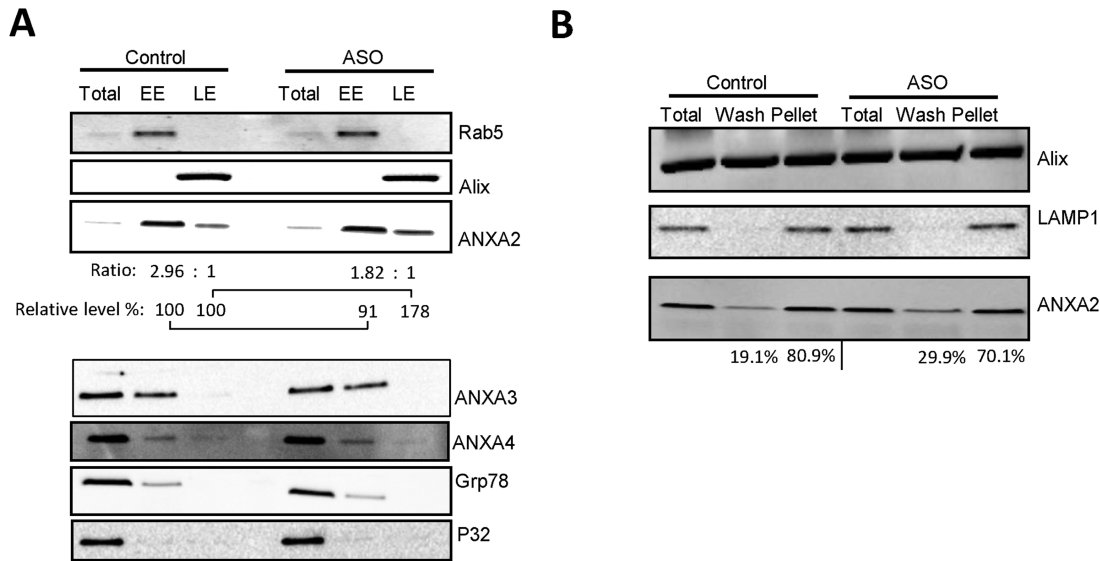
Figure 5. ANXA2 associated with LEs is resistant to high salt treatment. (**A**) Western analyses for proteins present in endosomal fractions isolated from A431 cells treated or not treated with 2 μM PS-ASO (IONIS ID 116847) for 16 hrs. Markers of EEs (Rab5), LEs (Alix), endoplasmic reticulum (Grp78), and mitochondria (P32) were evaluated. ANXA2, ANXA3 and ANXA4 were probed sequentially. The signal intensity of ANXA2, quantified using ImageJ, was reported relative to levels of Rab5 and Alix. The ANXA2 amounts were presented as a ratio of amounts in EE versus LE and as percentages in PS-ASO-treated cells compared to that in control cells. (**B**) LE fractions were treated with 2 M NaCl buffer for 30 min, and total, membrane pellet, and wash were analyzed by Western blotting. ANXA2 protein levels were quantified using ImageJ, normalized to Alix, and the relative levels of ANXA2 in the pellet and released fractions were given.

membrane conformation either from inside or outside of LEs to promote PS-ASO release.

PS-ASOs reduce target RNAs post release from LEs

Given that PS-ASOs are transported along the endocytotic pathway, PS-ASO release could occur either during the fusion process from early to late endosomes or after they are localized to LEs. To test these two possibilities, we first monitored how fast PS-ASOs exit from EEs and transport to LEs. Cells were stained with either EEA1 or Rab7a, markers of early and late endosomes, respectively, after they were treated with PS-ASOs for 20 or 40 min (Figure 7A, a, b and c). At 20 min, PS-ASOs were mainly co-localized with EEA1. At 40 min, PS-ASOs were predominantly observed in LEs, stained with Rab7a, indicating that PS-ASOs enter LEs from EEs within 20–40 min. Cells were also stained with LAMP1, a marker of LEs and lysosomes. Co-localization of PS-ASOs and LAMP1 was already observed at 40 min and significantly increased 1 hr after PS-ASO incubation (Figure 7A, d, e and f). Thus, trafficking of PS-ASOs from early to late endosomes takes less than 40 min.

We next performed a kinetic study on PS-ASO activity to dissect the contribution of early to late endosome fusion versus release from LEs to PS-ASO activity. Cells were treated with PS-ASOs for a short period of time and PS-ASO activity was monitored at different times after PS-ASO removal from the medium. If PS-ASO release had mainly occurred during the fusion process from early to late endosomes, the activity of PS-ASOs should have been maximized shortly after the PS-ASO removal, and the activity should not increase with prolonged incubation of PS-ASO,

since PS-ASO transport from early to late endosome occurs only within 40 mins. On the other hand, if PS-ASO productive release mainly occurs from LEs, PS-ASO activity should occur later and gradually increase over time after PS-ASOs were in LEs.

To test that, A431 cells were treated with PS-ASOs only for 2 hrs and ASO activities were then monitored at the time of PS-ASO removal and 4, 8 and 12 hrs after. Interestingly, PS-ASO activities (mRNA reduction) were not detected for either *Drosha* or *Malat1* until at least 4 hrs after the PS-ASO removal, and the activities increased over time and were not maximal until at least 12 hrs after the PS-ASO removal (Figure 7B), suggesting that the productive PS-ASO release occurs after PS-ASOs reach LEs. Altogether, our results show that target mRNA reduction fell significantly behind the time frame that PS-ASOs exited from EEs, indicating that PS-ASO becomes active mainly after it escapes from LEs but not during the fusion process from early to late endosomes.

Depletion of ANXA2 delays endocytic trafficking of PS-ASOs to LEs

ANXA2 regulates late endosomal biogenesis by mediating membrane invagination (28). We reasoned that ANXA2 might mediate PS-ASO transport from early to late endosomes. To test this possibility, we analyzed the transport of PS-ASOs in cells deficient in ANXA2. HeLa cells treated with *ANXA2*-specific siRNA for 48 hrs were incubated with 2 μM Cy3-labeled PS-ASO (IONIS ID 446654) for 2 hrs, and stained with EEA1 and Rab7a, markers of early and late endosomes, respectively. In addition, cells were stained with LAMP1 (data not shown), which is present in
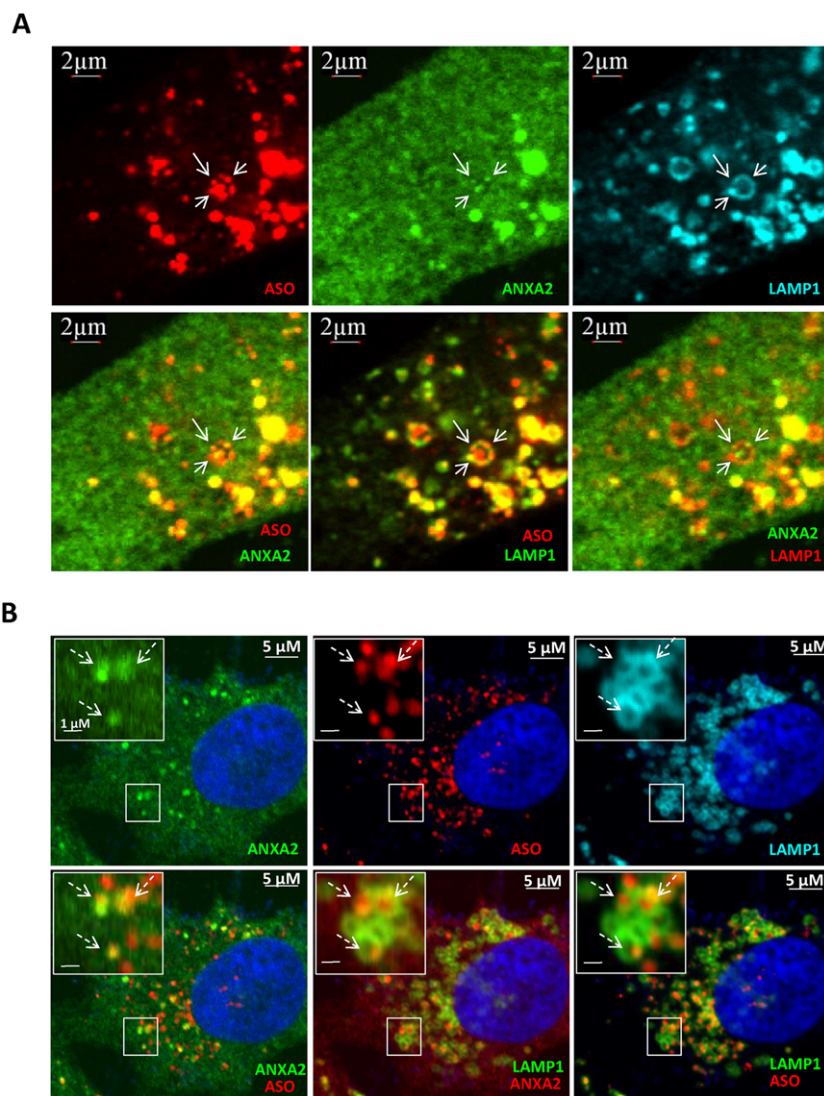
Figure 6. ANXA2 is present with PS-ASOs inside LEs. (**A**) HeLa cells incubated with 2 μM Cy3-PS-ASO (IONIS ID 446654) for 8 hrs were co-stained for ANXA2 and LAMP1. ANXA2 and PS-ASO in a LAMP1 enclosed structure are indicated by arrows. Scale bars, 2 μm. (**B**) HeLa cells were incubated with 2 μM Cy3-PS-ASO (IONIS ID 446654) for 8 hrs, and cells were treated with U18666A for an additional 16 hrs. Cells were co-stained with ANXA2 and LAMP1. Scale bars, 5 μm. For magnified areas, scale bars, 1 μm.

both LEs and lysosomes. Under this experimental condition, reduction of ANXA2 did not significantly alter the sizes of early and late endosomes (Figure 8A and B, left panels). Quantification of PS-ASO-positive EEs (PS-ASO and EEA1 co-staining), PS-ASO-positive LEs (PS-ASO and Rab7 co-staining), and PS-ASO-containing LAMP1-positive organelles showed that ANXA2 deficiency dramatically increased the portion of EEs that contained PS-ASOs and reduced numbers of PS-ASO-containing LEs and LAMP1-stained organelles (Figure 8C–E). The total numbers of EEA1-, Rab7-, LAMP1-stained organelles were not significantly altered in the absence of ANXA2 under this experimental condition (Figure 8F). These data indicate that trafficking of PS-ASOs from early to late endosomes was impaired in cells deficient in ANXA2. Since PS-ASO release mainly occurs from LEs, delayed traffic of PS-

ASOs to LEs could be attributable to decreased PS-ASO release from LEs due to ANXA2 reduction.

In addition, we further investigated the effect of the ANXA2 deficiency on other types of EEs, mainly recycling endosomes. Cells were stained with Rab11, marker of recycling endosome, after they were incubated with PS-ASOs. Rab11 does not primarily co-localize with PS-ASOs (Supplementary Figure S6A). ANXA2 reduction neither altered Rab11 localization nor co-localization pattern with PS-ASOs. Even knocking down Rab11 does not significantly affect PS-ASO activity (Supplementary Figure S6B and S6C). Therefore, these results exclude the possibility that recycling endosome plays an indispensable role in PS-ASO release for activity. These results also reinforce our conclusion that PS-ASOs mainly gain activity after they escape from LEs but not from recycling endosomes or during fusion process from early to late endosomes.
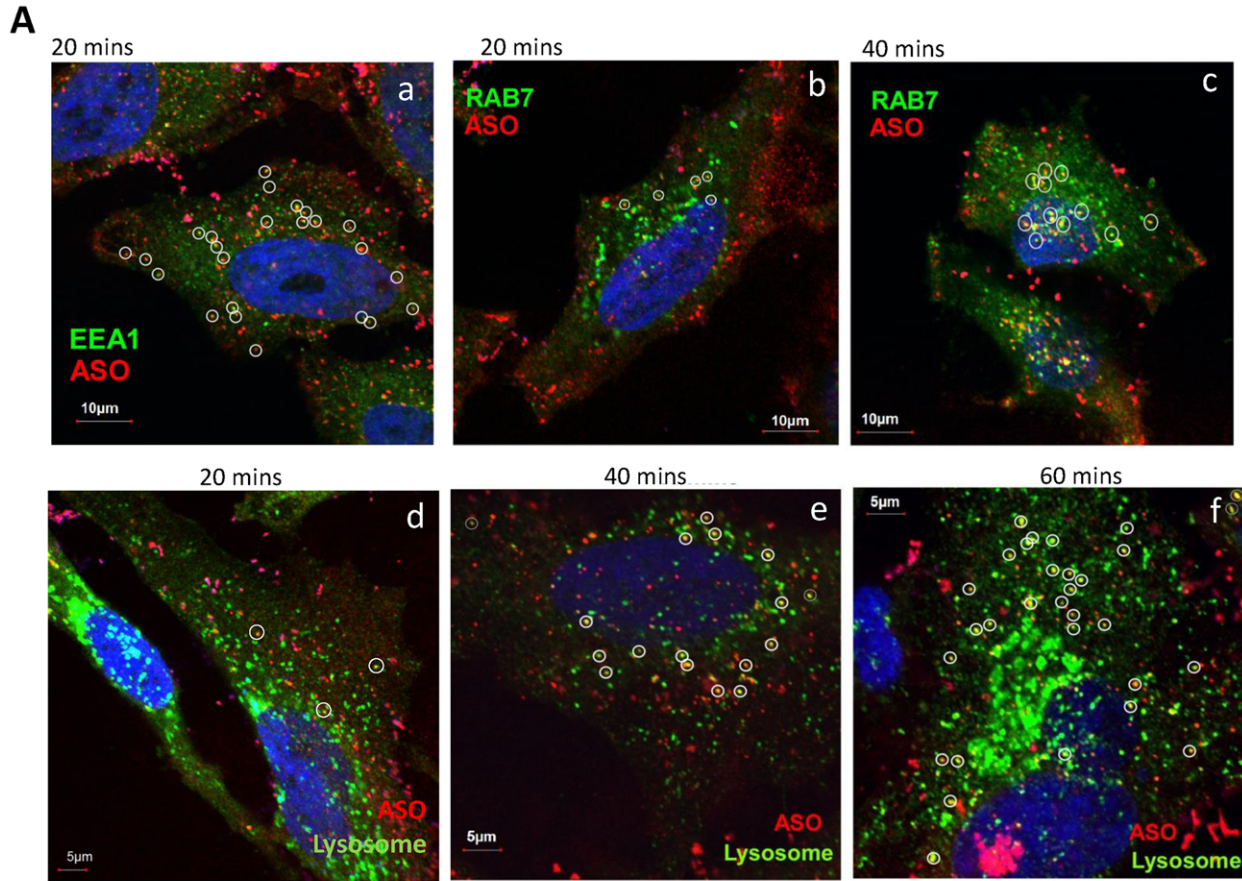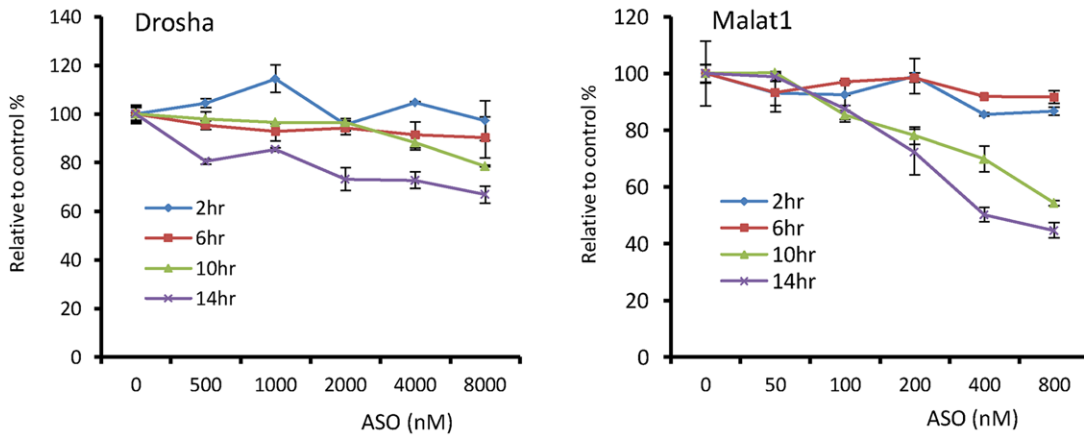
Figure 7. PS-ASOs gain activity after they escape from LEs. (**A**) Representative images of immunofluorescent staining for EEA1 (green in panel a), Rab7 (green in panel b and c), and LAMP1 (green in panel d, e and f) in HeLa cells incubated with Cy3-labeled PS-ASOs (IONIS ID 446654) for indicated times. Images for PS-ASO (red), EEA1, Rab7, and LAMP1 (green) were merged to show the co-localization, which were circled. The nuclei were stained with DAPI (blue). Scale bars are indicated. (**B**) Kinetic studies on PS-ASO activity for *Drosha* and *Malat1* RNA reduction. A431 cells were incubated with PS-ASOs targeting either *Drosha* or *Malat1* for 2 hrs after which PS-ASOs were removed. Cells were then collected at 2, 6, 10 and 14 hrs after PS-ASO treatment for activity assay and the RNA levels were quantified using qRT-PCR. The error bars represent standard deviations from three independent experiments.
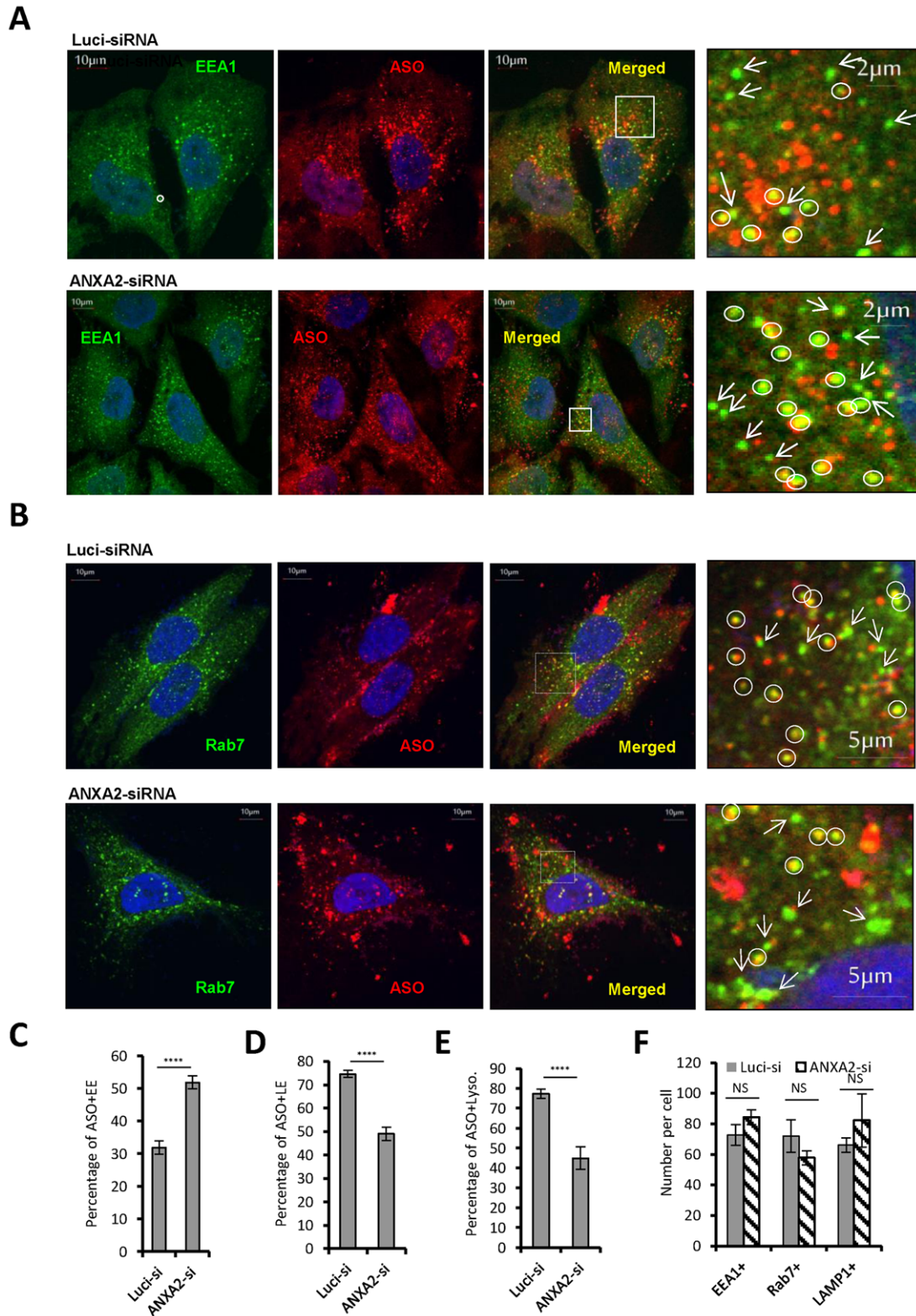
Figure 8. PS-ASO transport from early to late endosomes is impaired in ANXA2-deficient cells. (**A** and **B**) HeLa cells treated with a Luc-si or ANXA2-si for 48 hrs were incubated with 2 μM Cy3-PS-ASO (IONIS ID 446654) for 2 hrs, and co-stained with (A) EEA1 or (B) Rab7. The PS-ASO-positive EEA1- and Rab7-stained structures are circled; EEA1- and Rab7-stained loci that lack significant PS-ASO signals are indicated by arrows. Scale bars, 10 μm. In magnified regions shown in right panels, scale bars are indicated in the figures. (**C–E**) The PS-ASO-positive (C) EEs, (D) LEs, and (E) LAMP1-stained endosomes/lysosomes were counted in 15 cells and the percentage of the PS-ASO-positive organelles were calculated relative to the total numbers of the corresponding organelles. (**F**) The total numbers of the indicated organelles per cell. The error bars represent standard deviations. *P*-values were calculated based on unpaired *t*-test. $P < 0.0001$,****; N.S., not significant.
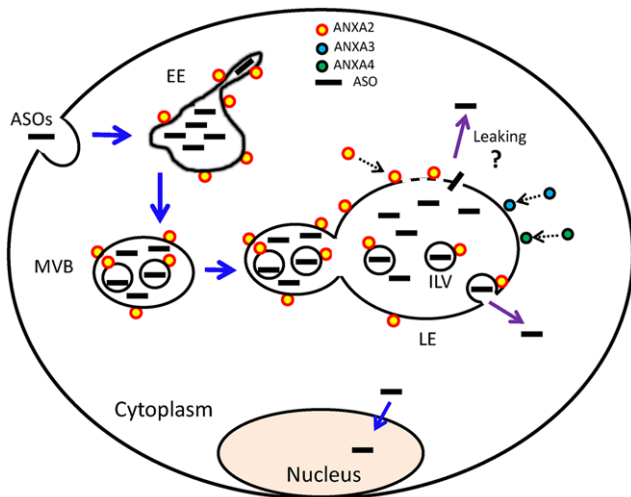
Figure 9. Proposed model of ANXA2-mediated PS-ASO trafficking and release. PS-ASOs (black lines) enter EEs where ANXA2 (yellow open circle) is present. ANXA2 mediates biogenesis of PS-ASO-containing MVBs. ANXA2 may bind PS-ASO-containing cargo to travel into MVBs or may be recruited to the late endosomal membrane as ANXA3 (blue open circle) and ANXA4 (green open circle) through interaction with lipids. PS-ASO release mainly occurs in MVBs/LEs. Early endosomal ANXA2 facilitates PS-ASO trafficking from early to late endosomes for PS-ASO release and late endosomal ANXA2 could mediate PS-ASO release at LEs.

Bafilomycin is an inhibitor of early to late endosome transport (36). We therefore treated cells with bafilomycin and then analyzed for ASO activity and ANXA2 localization. In cells treated with PS-ASOs, bafilomycin treatment blocked localization of ANXA2 to LEs and significantly reduced ASO activity (Supplementary Figure S7A and S7B). These observations are in line with the importance of ASO early to late endosome trafficking pathway in productive ASO release, which also reinforces the notion that ANXA2 could transport together with ASOs to LEs and facilitate ASO release from LEs. A proposed model to summarize ANXA2 functions in ASO intracellular trafficking and productive release was illustrated in Figure 9.

DISCUSSION

ANXA2 was previously identified as a PS-ASO-binding protein and was important for PS-ASO activity (15). In this study, we demonstrated that ANXA2 facilitates endocytic trafficking of PS-ASOs from early to late endosomes. The effect of ANXA2 on PS-ASO activity was observed in different cell types, indicating a common PS-ASO trafficking mechanism. ANXA2 was recruited to LEs in a time- and PS-ASO-concentration dependent manner, and ANXA2 reduction led to PS-ASO accumulation in EEs, which was coupled with the decreased PS-ASO activity. Both immunofluorescence staining and fractionation analyses showed that ANXA2 was present inside LEs in cells treated with PS-ASO, suggesting that ANXA2 may facilitate productive PS-ASO release from LEs into the cytoplasm.

It has been reported that ANXA2 is present at the plasma membrane and in the extracellular matrix (37), and we showed that ANXA2 is able to bind to PS-ASOs (15). The

data shown here indicate that ANXA2 does not affect PS-ASO internalization. In addition, we showed that the co-localization of ANXA2 and PS-ASO may not be mediated by direct binding because ANXA2 co-localized in LEs with a PO-ASO that does not significantly interact with ANXA2 protein. Thus, our results suggest that ANXA2 is important for PS-ASO activity by mediating PS-ASO intracellular trafficking. We note that reduction of ANXA2 did not completely block PS-ASO trafficking from early to late endosome. This may be caused by incomplete depletion of the protein, or that other redundant proteins/pathways might partially compensate the effect of reduction of ANXA2 on PS-ASO trafficking.

ANXA2 exists in cells as a monomer and in a heterotetrameric complex with S100A10. The effect of ANXA2 on PS-ASO activity appears to be independent of S100A10. Although S100A10 was also recruited to LEs upon treatment of cells with PS-ASO, depletion of S100A10 did not alter PS-ASO activity or ANXA2 localization to LEs. This indicates that the monomeric form of ANXA2 is important for PS-ASO activity. Consistent with this view, ANXA2 has been shown to function independently of S100A10 in EGF trafficking (29).

ANXA2 is required for the biogenesis of LEs. ANXA2 bridges between actin and the early endosomal membrane to facilitate membrane remodeling that accompanies endosome biogenesis (28). Depletion of ANXA2 strongly inhibits the formation of multiple vesicular bodies (MVBs) and the transport of dextran and EGF to LEs (25). ANXA2 localization to LEs was observed within an hour of PS-ASO addition to cells, and it appears that accumulation of ANXA2 in LEs is, at least partially due to co-transport with PS-ASO from EEs. Discreet, punctate co-localization of PS-ASO with ANXA2 was observed inside LEs, suggesting that these loci may exist as sub-structures within the lumen, likely as ILVs. ILVs form from luminal invaginations of the early endosomal membrane; these then detach to form free ILVs contained within the mature MVB (24). In vitro experiments have demonstrated a direct role for ANXA2 in ILV formation (7). Therefore, the transport of PS-ASOs from EEs to ILVs may recruit ILV-associated ANXA2 to LEs. It is interesting to note that in our fractionation experiments, a small but significant amount of ANXA2 was observed in LEs in non-PS-ASO treated cells. This suggests that transport of ANXA2 from early to late endosomes may be an intrinsic but active process. In cells not treated with PS-ASO, ANXA2 may be quickly released from LEs.

We observed ANXA2 inside LEs, but our experiments also showed that ANXA2 was bound to the surface of the endosomal membrane in the presence of PS-ASO. Although a significant fraction of ANXA2 was released from LE membrane by a high salt wash, the majority of ANXA2 in LE fraction was resistant to high salt treatment. We hypothesize that this fraction is inside endosomes, but it is also possible that the interaction between ANXA2 and membrane lipid is tight. It has been reported that ANXA2 can interact with the lipid raft region via a fairly strong interaction that might be difficult to disrupt (37). Accumulation of PS-ASOs in these organelles may cause changes in lipid composition or conformation that recruit ANXA2. The view that the lipid signature is altered upon PS-ASO treat-

ment is supported by the observations that ANXA3 and ANXA4 were also recruited to LEs upon PS-ASO treatment. Annexin family proteins prefer to bind negatively charged phospholipids and cholesterol as well (18). It is likely that with increased accumulation of PS-ASOs in LEs, changes in the membrane structure or lipid components occur (2), which reveal annexin binding sites.

Importantly, ANXA2 is required for normal PS-ASO activity, suggesting that ANXA2 facilitates PS-ASO trafficking via the productive pathway. ANXA2 may both mediate PS-ASO transport from early to late endosomes, and facilitate PS-ASO release from the membrane-enclosed organelles (Figure 9). It has been proposed that productive PS-ASO release occurs due to leakage during membrane fusion or fission when a single-layer lipid membrane is formed (10). Our kinetic studies suggest that substantial productive PS-ASO release does not occur during fusion process from early to late endosomes but after PS-ASOs reach LEs. Thus, it is likely that productive PS-ASO release from LEs is dependent on appropriate ASO migration from early to late endosomes, which process requires ANXA2. Free uptake in *in vitro* cell culture system may not correlate with *in vivo* uptake, thus the functional role of ANXA2 in PS-ASO activity *in vivo* needs further investigation.

PS-ASO release from LEs has been proposed to occur via a process mediated by lipid flip-flops (8,38). Some small molecules, such as Ritro-1, dramatically enhance PS-ASO release from LEs and PS-ASO activity (39), indicating that PS-ASO release from LEs significantly contributes to PS-ASO activity. Our data support the hypothesis that ANXA2 facilitates PS-ASO release from LEs. Given that ANXA2 can interact with membrane lipids and is able to induce lipid segregation and membrane budding (24), membrane surface-associated ANXA2 may alter the permeability allowing PS-ASO release from LEs (Figure 9). The amphipathic helical structure of ANXA2 has been reported to sense lipid packing defects or increased membrane curvature (40); these defects may result from the presence of PS-ASO in LEs. ANXA2 association with such sites may further increase the curvature and potentiate PS-ASO release. Understanding the mechanism of productive PS-ASO release in greater detail remains an important issue as it will guide development of PS-ASO modifications or formulations that enhance the pharmacological effects of PS-ASOs (41).

SUPPLEMENTARY DATA

Supplementary Data are available at NAR Online.

ACKNOWLEDGEMENTS

FUNDING

REFERENCES

1. Crooke,S.T. (2004) Progress in antisense technology. *Annu. Rev. Med.*, **55**, 61–95.
2. Juliano,R.L., Ming,X. and Nakagawa,O. (2012) Cellular uptake and intracellular trafficking of antisense and siRNA oligonucleotides. *Bioconjugate Chem.*, **23**, 147–157.
3. Koller,E., Vincent,T.M., Chappell,A., De,S., Manoharan,M. and Bennett,C.F. (2011) Mechanisms of single-stranded phosphorothioate modified antisense oligonucleotide accumulation in hepatocytes. *Nucleic Acids Res.*, **39**, 4795–4807.
4. Bennett,C.F. and Swayze,E.E. RNA targeting therapeutics: molecular mechanisms of antisense oligonucleotides as a therapeutic platform. *Annu. Rev. Pharmacol. Toxicol.*, **50**, 259–293.
5. Beltinger,C., Saragovi,H.U., Smith,R.M., LeSauteur,L., Shah,N., DeDionisio,L., Christensen,L., Raible,A., Jarett,L. and Gewirtz,A.M. (1995) Binding, uptake, and intracellular trafficking of phosphorothioate-modified oligodeoxynucleotides. *J. Clin. Invest.*, **95**, 1814–1823.
6. Prakash,T.P., Graham,M.J., Yu,J., Carty,R., Low,A., Chappell,A., Schmidt,K., Zhao,C., Aghajan,M., Murray,H.F. *et al.* (2014) Targeted delivery of antisense oligonucleotides to hepatocytes using triantennary N-acetyl galactosamine improves potency 10-fold in mice. *Nucleic Acids Res.*, **42**, 8796–8807.
7. Scott,C.C., Vacca,F. and Gruenberg,J. (2014) Endosome maturation, transport and functions. *Semin. Cell Dev. Biol.*, **31**, 2–10.
8. Juliano,R.L. and Carver,K. (2015) Cellular uptake and intracellular trafficking of oligonucleotides. *Adv. Drug Deliv. Rev.*, **87**, 35–45.
9. Juliano,R.L., Ming,X., Carver,K. and Laing,B. (2014) Cellular uptake and intracellular trafficking of oligonucleotides: implications for oligonucleotide pharmacology. *Nucleic Acid Ther.*, **24**, 101–113.
10. Varkouhi,A.K., Scholte,M., Storm,G. and Haisma,H.J. (2011) Endosomal escape pathways for delivery of biologicals. *J. Controlled Release*, **151**, 220–228.
11. Blumenthal,R., Clague,M.J., Durell,S.R. and Epand,R.M. (2003) Membrane fusion. *Chem. Rev.*, **103**, 53–69.
12. Wickner,W. and Schekman,R. (2008) Membrane fusion. *Nat. Struct. Mol. Biol.*, **15**, 658–664.
13. Martens,S. and McMahon,H.T. (2008) Mechanisms of membrane fusion: disparate players and common principles. *Nat. Rev. Mol. Cell Biol.*, **9**, 543–556.
14. Frolov,V.A., Dunina-Barkovskaya,A.Y., Samsonov,A.V. and Zimmerberg,J. (2003) Membrane permeability changes at early stages of influenza hemagglutinin-mediated fusion. *Biophys. J.*, **85**, 1725–1733.
15. Liang,X.H., Sun,H., Shen,W. and Crooke,S.T. (2015) Identification and characterization of intracellular proteins that bind oligonucleotides with phosphorothioate linkages. *Nucleic Acids Res.*, **43**, 2927–2945.
16. Liang,X.H., Shen,W., Sun,H., Prakash,T.P. and Crooke,S.T. (2014) TCP1 complex proteins interact with phosphorothioate oligonucleotides and can co-localize in oligonucleotide-induced nuclear bodies in mammalian cells. *Nucleic Acids Res.*, **42**, 7819–7832.
17. Shen,W., Liang,X.H. and Crooke,S.T. (2014) Phosphorothioate oligonucleotides can displace NEAT1 RNA and form nuclear paraspeckle-like structures. *Nucleic Acids Res.*, **42**, 8648–8662.
18. Gerke,V. and Moss,S.E. (2002) Annexins: from structure to function. *Physiol. Rev.*, **82**, 331–371.
19. Flower,R.J. and Perretti,M. (2015) 'Annexins' themed section. *Br. J. Pharmacol.*, **172**, 1651–1652.
20. Lizarbe,M.A., Barrasa,J.I., Olmo,N., Gavilanes,F. and Turnay,J. (2013) Annexin-phospholipid interactions. Functional implications. *Int. J. Mol. Sci.*, **14**, 2652–2683.
21. Patel,D.R., Isas,J.M., Ladokhin,A.S., Jao,C.C., Kim,Y.E., Kirsch,T., Langen,R. and Haigler,H.T. (2005) The conserved core domains of annexins A1, A2, A5, and B12 can be divided into two groups with different Ca2+-dependent membrane-binding properties. *Biochemistry*, **44**, 2833–2844.
22. Montaville,P., Neumann,J.M., Russo-Marie,F., Ochsenbein,F. and Sanson,A. (2002) A new consensus sequence for phosphatidylserine recognition by annexins. *J. Biol. Chem.*, **277**, 24684–24693.
23. Patel,D.R., Jao,C.C., Mailliard,W.S., Isas,J.M., Langen,R. and Haigler,H.T. (2001) Calcium-dependent binding of annexin 12 to

phospholipid bilayers: stoichiometry and implications. *Biochemistry*, **40**, 7054–7060.

24. Drucker,P., Pejic,M., Galla,H.J. and Gerke,V. (2013) Lipid segregation and membrane budding induced by the peripheral membrane binding protein annexin A2. *J. Biol. Chem.*, **288**, 24764–24776.

25. Mayran,N., Parton,R.G. and Gruenberg,J. (2003) Annexin II regulates multivesicular endosome biogenesis in the degradation pathway of animal cells. *EMBO J.*, **22**, 3242–3253.

26. Thiel,C., Osborn,M. and Gerke,V. (1992) The tight association of the tyrosine kinase substrate annexin II with the submembranous cytoskeleton depends on intact p11- and Ca(2+)-binding sites. *J. Cell Sci.*, **103**, 733–742.

27. MacLeod,T.J., Kwon,M., Filipenko,N.R. and Waisman,D.M. (2003) Phospholipid-associated annexin A2-S100A10 heterotetramer and its subunits: characterization of the interaction with tissue plasminogen activator, plasminogen, and plasmin. *J. Biol. Chem.*, **278**, 25577–25584.

28. Morel,E., Parton,R.G. and Gruenberg,J. (2009) Annexin A2-dependent polymerization of actin mediates endosome biogenesis. *Dev. Cell*, **16**, 445–457.

29. de Graauw,M., Cao,L., Winkel,L., van Miltenburg,M.H., le Devedec,S.E., Klop,M., Yan,K., Pont,C., Rogkoti,V.M., Tijsma,A. *et al.* (2014) Annexin A2 depletion delays EGFR endocytic trafficking via cofilin activation and enhances EGFR signaling and metastasis formation. *Oncogene*, **33**, 2610–2619.

30. Crooke,S.T. (2004) Antisense strategies. *Curr. Mol. Med.*, **4**, 465–487.

31. Zobiack,N., Rescher,U., Ludwig,C., Zeuschner,D. and Gerke,V. (2003) The annexin 2/S100A10 complex controls the distribution of transferrin receptor-containing recycling endosomes. *Mol. Biol. Cell*, **14**, 4896–4908.

32. Brandherm,I., Disse,J., Zeuschner,D. and Gerke,V. (2013) cAMP-induced secretion of endothelial von Willebrand factor is regulated by a phosphorylation/dephosphorylation switch in annexin A2. *Blood*, **122**, 1042–1051.

33. Morel,E. and Gruenberg,J. (2007) The p11/S100A10 light chain of annexin A2 is dispensable for annexin A2 association to endosomes and functions in endosomal transport. *PLoS One*, **2**, e1118.

34. Morel,E. and Gruenberg,J. (2009) Annexin A2 binding to endosomes and functions in endosomal transport are regulated by tyrosine 23 phosphorylation. *J. Biol. Chem.*, **284**, 1604–1611.

35. Sparrow,S.M., Carter,J.M., Ridgway,N.D., Cook,H.W. and Byers,D.M. (1999) U18666A inhibits intracellular cholesterol transport and neurotransmitter release in human neuroblastoma cells. *Neurochem. Res.*, **24**, 69–77.

36. Mallard,F., Antony,C., Tenza,D., Salamero,J., Goud,B. and Johannes,L. (1998) Direct pathway from early/recycling endosomes to the Golgi apparatus revealed through the study of shiga toxin B-fragment transport. *J. Cell Biol.*, **143**, 973–990.

37. Valapala,M. and Vishwanatha,J.K. (2011) Lipid raft endocytosis and exosomal transport facilitate extracellular trafficking of annexin A2. *J. Biol. Chem.*, **286**, 30911–30925.

38. Zelphati,O. and Szoka,F.C. Jr (1996) Mechanism of oligonucleotide release from cationic liposomes. *Proc. Natl. Acad. Sci. U.S.A.*, **93**, 11493–11498.

39. Yang,B., Ming,X., Cao,C., Laing,B., Yuan,A., Porter,M.A., Hull-Ryde,E.A., Maddry,J., Suto,M., Janzen,W.P. *et al.* (2015) High-throughput screening identifies small molecules that enhance the pharmacological effects of oligonucleotides. *Nucleic Acids Res.*, **43**, 1987–1996.

40. Antonny,B. (2011) Mechanisms of membrane curvature sensing. *Annu. Rev. Biochem.*, **80**, 101–123.

41. Ming,X., Carver,K., Fisher,M., Noel,R., Cintrat,J.C., Gillet,D., Barbier,J., Cao,C., Bauman,J. and Juliano,R.L. (2013) The small molecule Retro-1 enhances the pharmacological actions of antisense and splice switching oligonucleotides. *Nucleic Acids Res.*, **41**, 3673–3687.